Preparation of single-phase C–S–H specimens from hydrated tricalcium silicate pastes

Jeffrey J. Chen[a], Jeffrey J. Thomas[b], and Hamlin M. Jennings[ab*]
[a]Northwestern University, Department of Materials Science and Engineering, Evanston, IL 60208
[b]Northwestern University, Department of Civil and Environmental Engineering, Evanston, IL 60208

[*]Corresponding author: Tel: +1–847–491–4858, Fax: +1–847–491–4011
Email addresses jjchen@alumni.princeton.edu (J.J. Chen), h-jennings@northwestern.edu (H.M. Jennings)

Keywords: Calcium silicate hydrate (C–S–H), characterization, leaching, degradation

Abstract. Although the preparation of single-phase C–S–H specimens is usually from the reaction of CaO and SiO_2 or from the double decomposition of a Ca-salt and an alkali silicate in aqueous solution, recent evidence in the literature shows that these 'synthetic' preparations (especially double decomposition) produce nanostructures at high Ca/Si ratios quite different than that of C–S–H gel formed in mature C_3S or cement paste. These differences are most clearly evident from the fact that C–S–H gel has a maximum Ca/Si ratio of 1.7–1.8 while that of synthetic C–S–H is generally near 1.5. In this study, a methodology for preparing homogeneous, single-phase specimens of C–S–H gel from fully-hydrated C_3S paste is presented. The Ca/Si ratio of these specimens, which can vary between approximately 0.7–1.8, can be decreased and increased by careful decalcification (in concentrated NH_4NO_3 solution) and recalcification (in $Ca(OH)_2$ solution), respectively; the latter process is also shown to remove the compositional gradients in a leached solid, thereby enhancing the homogeneity of the specimen. This preparation technique is therefore valuable for structural studies of C–S–H gel at low Ca/Si ratios (which are prevalent in chemically degraded or blended cement pastes) and especially at high Ca/Si ratio, where the structure of C–S–H gel is most controversial.

1. Introduction

1.1. C–S–H gel versus 'synthetic' C–S–H. The principal product at room temperature in the paste hydration of tricalcium silicate (C_3S), the major constituent phase of portland cement, is a particular calcium silicate hydrate known as C–S–H gel. Determination of the structure of this compound is complicated by the lack of long-range order, by variation in composition at a submicron scale, and by the potential admixture with portlandite and unreacted C_3S. To obtain more homogeneous specimens, the majority of structural studies (e.g., [1-7]) have used single-phase or 'synthetic' C–S–H prepared by combining CaO and SiO_2 or by reacting an alkali silicate with a Ca-salt (i.e., double decomposition) in aqueous solution. In both preparations, the Ca/Si ratio of C–S–H is easily controlled by altering the initial molar ratio of CaO to SiO_2 from 0.7 to a maximum near 1.5. This method is useful and widely exploited, since arguably the most effective strategy for understanding the structural variations in C–S–H is to analyze the systematic changes in C–S–H with varying Ca/Si ratio.

Our recent studies [8-10] represent some of the first efforts to directly examine the variations in structure at different Ca/Si ratios of C–S–H gel formed in a fully-hydrated C_3S paste. Phase equilibrium results [8] illustrate important structural differences at high Ca/Si ratios between mature C–S–H gel and

synthetic C–S–H (especially that from double decomposition): the former has a higher maximum Ca/Si ratio of 1.8 (compared to 1.5), and, at a given Ca/Si ratio above 1.2, a higher mean silicate chain length and a higher Ca–OH content. From these results, it was concluded [8] that at high Ca/Si ratios, the structures of mature C–S–H gel and synthetic C–S–H more closely resemble degenerate forms of the minerals jennite [11] and tobermorite [12], respectively. It thus appears that synthetic preparations of C–S–H are inappropriate structural models for mature C–S–H gel at high Ca/Si ratios. Consequently, further insight into the nanostructure of C–S–H gel should be obtained from studies on single-phase C–S–H gel specimens that are derived from C_3S pastes and prepared at different Ca/Si ratios.

1.2 Decalcification of C_3S pastes. The hydration of a C_3S paste produces $Ca(OH)_2$ (CH) and a C–S–H gel with a mean Ca/Si ratio of 1.7–1.8, which is approximately invariant with age [13]. Several methods are available to prepare single-phase C–S–H specimens of varying Ca/Si ratio from C_3S: (1) C_3S can be hydrated in dilute suspensions at Ca concentrations below the saturation concentration of CH [14]; this suppresses the precipitation of CH and shifts the equilibrium Ca/Si ratio of C–S–H to lower values. (2) C_3S pastes can be hydrated with a sufficiently high content of silica fume (or other silica rich reactive component) [15-18], which will ultimately consume CH (via the pozzolanic reaction) and form C–S–H with lower Ca/Si ratios. (3) C_3S pastes can be hydrated to maturity then carefully leached to remove CH and, if desired, to decalcify C–S–H gel. Only the last of these three options allows for a C_3S paste hydration with normal kinetics and solution chemistry; this option is thus investigated here.

The simplest way to leach a cement paste is through continuous exposure to deionized water. However, the kinetics of this reaction are inconveniently slow: based on the findings of Carde et al. [19], a leaching front induced by flowing water will propagate only 1 mm through a cement paste of water:cement ratio = 0.50 in the span of 70 d and ~ 2.3 mm in 1 year. Organic solvents such as ethyl acetoacetate or glycerol-alcohol mixtures are also known to leach CH and C–S–H [20-25], but the possible contamination of C–S–H by these solvents has not been fully addressed, and the leaching of C–S–H below Ca/Si ~ 1.25 is sometimes difficult [25]

Accelerated alternatives to leaching in flowing water have been explored [19, 26, 27]. A particularly effective method is the use of concentrated NH_4NO_3 solutions [19, 28, 29]. The dissolution of CH by this method proceeds as,

$$Ca(OH)_2 + 2NH_4NO_3 \_ Ca^{2+} + 2OH^- + 2H^+ + 2NH_3 + 2NO_3^- \_ Ca^{2+} + 2NO_3^- + NH_3(g) + 2H_2O$$

where the reaction is driven to the right by the elimination of ammonium from the system as gaseous ammonia [29]. The resulting solubility of Ca in a 6 M NH_4NO_3 solution (2.9 M) is 2 orders of magnitude greater than that in water (20.6 mM). This ensures a high concentration gradient at the solid-liquid interface, thereby increasing the rate of leaching by a factor of approximately 100 [19] to 300 [29]. At equal degrees of leaching, Carde et al. [19] showed no significant differences in NH_4NO_3- or water-leached solids in terms of porosity, strength, microprobe analysis of major and minor elements, and XRD patterns. The absence of undesirable side reactions associated with NH_4NO_3 solutions is further confirmed by phase equilibrium and ^{29}Si NMR results on C–S–H [8], which show agreement between samples leached in water and NH_4NO_3 solution.

In the same phase equilibrium study [8], it was also shown that, as long as compositional gradients are minimized, decalcification and recalcification (i.e., the process of chemically incorporating Ca into a decalcified solid) are reversible processes; that is, the same structure of C–S–H is obtained whether

approaching equilibrium through the decalcification of a high Ca/Si ratio solid or through the recalcification of a low Ca/Si ratio solid. Consequently, if high Ca/Si ratio solids, originally prepared by two distinctly different methods such as the paste hydration of C_3S and the double decomposition of calcium nitrate and sodium silicate, are decalcified and then recalcified, the differences in structure that were initially detectable at high Ca/Si ratio (but too small to distinguish at low Ca/Si ratios) will clearly reemerge after recalcification. This 'memory' in the structure of C–S–H will be exploited here when preparing C–S–H gel specimens at Ca/Si ratios exceeding 1.5.

In this study, it is shown that single-phase C–S–H specimens can be prepared with varying Ca/Si ratio by decalcifying thin (0.8 mm) discs of fully-hydrated C_3S paste (water:cement = 0.5) in 6 M NH_4NO_3 solution. A procedure for enhancing the homogeneity of these samples and for preparing specimens at high Ca/Si ratio is also reported.

2. Experimental

2.1. Samples. C_3S pastes, prepared at a water:cement ratio of 0.5, were hydrated for 8 months, at which point the samples were nearly completely reacted; see Ref. [8] for further details. Immediately prior to leaching (Section 2.2), pastes were cut with a diamond saw into discs, approximately 0.8 mm thick and 25 mm in diameter.

2.2. Decalcification in 6 M NH_4NO_3 solution. A C_3S paste was decalcified by immersing one saturated 0.8-mm thick disc in a stirred 100-mL solution of 6 M NH_4NO_3. Based on the weight of dry solid, the solution:solid weight ratio was ~ 200. The weight of the sample (measured in the saturated surface dry state) was monitored during leaching; at the desired weight loss, the sample was removed from the NH_4NO_3 solution and immediately immersed in ~ 50 mL of deionized water to remove the residual NH_4NO_3 solution residing in the pores of the paste. A series of decalcified C_3S pastes were prepared in this way. As confirmed by pore fluid exchange calculations [30], approximately 10–15 min of gentle stirring in deionized water was sufficient for complete replacement of the heavier NH_4NO_3 solution (ρ ~ 1.13 g cm^{-3}) by water.

Bulk Ca/Si ratios of the leached pastes were measured by ICP after decomposition of the solid with $LiBO_3$ at 1000 ºC [31]. For several samples, the Ca and Si concentrations in the NH_4NO_3 solutions were measured by ICP after leaching.

2.3 Recalcification of leached samples. The process of chemically incorporating Ca into a leached solid is referred to here as recalcification. In this study, a recalcified sample was examined by SEM-EDX (Section 2.5). This sample, initially a fragment (~ 0.2 g, saturated) of a C_3S paste leached in NH_4NO_3 solution to a Ca/Si ratio of 0.83, was shaken for three weeks with 30 mL of a solution initially containing 24 mM Ca; the solution:solid weight ratio was ~ 300. At the end of this period, the Ca/Si ratio of the recalcified solid was 1.31, and the composition of the solution was equilibrated on solubility curve C of Figure 10 in Ref. [8] at [Ca] = 7.06 mM Ca, [Si] = 71.3 μM. The CH solution was prepared with deionized water, and CaO was obtained from freshly decomposed $CaCO_3$.

2.3. Quantitative X-ray diffraction analysis (QXDA). To determine the bulk Ca/Si ratio at which CH was fully extracted from the paste, the content of CH in a series of decalcified C_3S pastes was measured

by QXDA using corundum (α-Al_2O_3) as an internal standard (α-Al_2O_3:sample = 2:5). Scans were acquired with a Rigaku X-ray diffractometer with CuKα radiation operating at 40 kV and 20 mA, stepping 0.75° 2θ·min^{-1} over the range 5°–60° 2θ. The analysis used the area intensities of 3–5 peaks of CH and of 5 peaks for α-Al_2O_3. Each sample was thus associated with up to 25 ratios of these intensities, from which an average CH content was computed. Assuming complete hydration and negligible carbonation (no $CaCO_3$ was detected by XRD), this CH content was used to compute the Ca/Si ratio of C–S–H in the paste.

2.4. SEM X-ray microanalysis (EDX). To determine the compositional homogeneity of a sample, the Ca/Si ratios were measured by SEM-EDX across the thickness of a leached and recalcified disc; the latter (Ca/Si = 1.31) was initially a fragment of a leached disc (Ca/Si = 0.83) (see Section 2.3).

A Hitachi-3500 SEM equipped with a W hairpin filament and PGT energy dispersive X-ray analyzer was used. Microanalyses were made at an accelerating voltage of 10 keV, a counting time of 60 s, and a probe current, measured by a Faraday cup, of 1.30 ± 0.01 nA. Pseudo-wollastonite (α-$CaSiO_3$) was used as a reference standard, and matrix corrections were made by the Phi-Rho-Z method.

Results are reported as a function of the distance from the surface. In each sample, 2–3 random traverses were made, each with incremental steps of 30 μm; 2 of the 3 traverses were staggered by 15 μm to sample more distances.

2.5. Porosity and density. The bulk wet density (ρ_b) of the 0.8-mm thick sample discs were determined by measuring the external dimensions of the disc with digital calipers and by carefully weighing the saturated, surface-dried sample to the nearest 0.0001 g.

The porosity (ϕ) of the sample was determined by dividing the volume of water evaporated after D-drying [32] for 5–7 days by the volume of the sample disc. The density of the evaporated liquid is assumed to be 1 g cm^{-3}. This value may be slightly underestimated, as some of the water lost on D-drying will remove more firmly condensed water such as that found in the interlayer spaces of C–S–H [33, 34]. Nevertheless, the inaccuracies attributed to the assumption will not alter the observed trends.

3. Results

3.1. Leaching in NH_4NO_3 solution: general observations and kinetics. Except for a slight transparency at high degrees of leaching, the C_3S pastes did not show any visible signs of deterioration during leaching in NH_4NO_3 solution. This was true even after a sample disc lost 38% of its original saturated mass (or nearly 70% of its solid mass[†]), by which time the Ca/Si ratio of the C_3S paste had decreased to 0.17 and the porosity had exceeded 80% (Section 3.6). At these high degrees of leaching, samples were fragile but still strong enough to have its external dimensions measured with calipers as reported elsewhere [35].

Due to the high solubility of Ca, the rate of decalcification of cement pastes is greatly accelerated in 6 M NH_4NO_3 when compared to that in water. Figure 1 shows the kinetics of leaching a C_3S paste in 6 M NH_4NO_3 and a Type I white portland cement (WPC) paste (water:cement = 0.5) in flowing deionized water (described elsewhere [35]); plotted against time are the changes in the bulk Ca/Si ratio of the paste

[†] This discrepancy arises since the solid leached from the paste will be replaced by an equal volume of water; consequently, the measured weight loss of the saturated paste will be lower than the actual weight loss of the solid.

(measured from correlations with weight loss as described in Section 3.4). Although the comparison between the leached C_3S and WPC pastes is only qualitative (since the latter also contains aluminate phases such as ettringite), it is still illustrative since the specimen sizes are identical and the initial Ca/Si ratio of both pastes is 3. Consistent with estimates derived from measured propagation rates of leaching fronts [19, 29], the results in Figure 1 show that exposure of hardened pastes to 6 M NH_4NO_3 solution leads to an acceleration in leaching by over 2 orders of magnitude. For example, to leach a paste from a Ca/Si of 3 to 1.25 requires 16.2 x 10^3 min (11.3 days) of leaching in water while only 49 min in 6 M NH_4NO_3.

3.2. Ca and Si concentrations in NH_4NO_3 leaching solutions. Figure 2 shows the final Ca and Si concentrations in NH_4NO_3 solutions after leaching a series of C_3S pastes; each pair of points at a given bulk Ca/Si ratio represents the concentrations in a different 100-mL solution after the leaching of a single specimen disc. The linearly increasing Ca concentration and the nearly zero Si concentration in solution with decreasing solid Ca/Si ratio indicates that the predominant element leached from the solid is Ca. The loss in Si is negligible even below a solid Ca/Si ratio of 1, the approximate composition below which the equilibrium concentration of Si in water exceeds that of Ca [8]; thus, unlike in water, leaching in NH_4NO_3 solution is nearly a pure decalcification. This conclusion is further supported by the agreement between the measured Ca concentrations and the computed curve in Figure 2, which assumes the decrease in the solid Ca/Si ratio is solely from the loss of Ca.

The significance of a pure decalcification in NH_4NO_3 solution is twofold. (1) It allows decalcification of C_3S or cement pastes below Ca/Si ~ 1–1.2, compositions that would otherwise be difficult or slow to achieve by leaching in pure water. Although C–S–H gel phases with these low Ca/Si ratios are generally absent in normal cement pastes, the study of them is important since they could be present in water-, sulfate-, or carbonation-attacked pastes and in pastes blended with a high content of mineral additions; moreover, below a Ca/Si ratio of 1.2, C–S–H gel begins to show important changes in nanostructure, the most prominent being increases in silicate polymerization and silanol content [8] and decreases in specific surface area [10]. (2) A pure decalcification process also minimizes the loss of Si from the solid, indicating that entire regions of the paste are not lost to solution as would occur by dissolution and erosion during a flowing water experiment; this conclusion is consistent with the lack of visibly eroded edges in the NH_4NO_3-leached samples. The minimization of erosion is important when measuring the dimensional changes caused by intrinsic structural changes in the paste induced by decalcification [35].

3.3 Removal of CH and decalcification of C–S–H. Figure 3 shows the distribution of phases and the Ca/Si ratio of C–S–H as a function of the bulk Ca/Si ratio of the paste decalcified in NH_4NO_3 solution. The dashed line (with a slope of 1) represents the Ca/Si ratio of the paste; the solid line is a best-fit curve for the Ca/Si ratios of C–S–H computed from CH contents measured by QXDA. The intersection of the two lines at a Ca/Si ratio of approximately 1.4 marks the composition of the paste (and of C–S–H) at which CH (represented by the vertically-hatched area) is initially removed from the paste by decalcification. The slight decrease in the Ca/Si ratio from about 1.7 to 1.4 before this intersection indicates that the initial stages of decalcification of C–S–H gel occurred simultaneously with the dissolution of CH. This overlap (which is strictly absent under ideal equilibrium conditions) is thought to be primarily due to compositional gradients across the 0.8-mm thickness of the specimen (see Section

3.5). As illustrated in Section 3.5, these compositional gradients can be eliminated by recalcifying the leached specimen in CH solution.

XRD shows that amorphous silica gel is only present at very low Ca/Si ratios and that C–S–H is the sole phase present in our NH_4NO_3-leached samples between Ca/Si ratios of 0.7–1.4 [8].

3.4. Correlations between weight loss and Ca/Si ratio of C_3S pastes. When preparing single-phase C–S–H specimens through the decalcification of C_3S pastes, it is useful to know the Ca/Si ratio of the solid during the leaching process. This can be accomplished directly by analyzing the composition of the solid or indirectly by analyzing the concentrations in the leaching solution at various times, but an alternative and somewhat simpler method is to use predetermined relationships between the solid Ca/Si ratio and the weight loss during leaching. Figure 4 shows such relationships for a C_3S paste leached in 6 M NH_4NO_3. The weight loss values associated with the solid curve in Figure 4 were determined from the percentage difference between the mass of the initial paste saturated with pore solution and the mass of the decalcified paste saturated with 6 M NH_4NO_3; the Ca/Si ratios were determined analytically on individual samples. The solid trendlines in Figure 4 were used in this study to compute the Ca/Si ratios in Figure 1 and in a related study [35] to correlate the Ca/Si ratio with the shrinkage strains in a C_3S paste during decalcification. Note that these trendlines are only valid for C_3S pastes prepared at a water:cement ratio of 0.5 and leached in 6 M NH_4NO_3 solution.

After a C_3S paste has reached its target Ca/Si ratio, it should be rinsed in deionized water (10–15 minutes is sufficient) to remove the residual NH_4NO_3 solution from the pores of the paste. This rinsing step results in an additional loss in weight since the 6 M NH_4NO_3 solution ($\rho \sim 1.13$ g cm^{-3}) is appreciably denser than that of water; the resulting weight loss-Ca/Si ratio curve for water-saturated leached samples (dashed lines in Figure 4) thus shifts to the right. Moreover, since the density of the pore solution of the initial, unleached C_3S paste is approximately that of water, this shifted curve more accurately represents the true weight loss of the saturated C_3S paste required to achieve a given Ca/Si ratio.

Both curves in Figure 4 show two linear regions that intersect at a bulk Ca/Si ratio of ~ 1.4. Since this composition was determined from QXDA (Section 3.3) to be that at which CH is completely removed from the C_3S paste, the first linear region (at lower weight loss) is associated primarily with the extraction of CH and the second with the decalcification of C–S–H. The assignment of the first linear region is supported by the initial slope of the water-saturated (dotted) line, –0.093, which is close to the theoretical value, –0.086, expected if the changes in weight and Ca/Si ratio were only due to the replacement of CH with an equal volume of water [30]. The assignment of the second linear region (with a more gradual slope of –0.065) to the decalcification of C–S–H is supported indirectly by the fact that blended cement pastes that lack CH exhibit only a single linear region of relatively gradual slope [35].

3.5. EDX-SEM. Previous studies [19, 29] have shown in samples larger than those studied here that, like leaching in water, decalcification in concentrated NH_4NO_3 solution produces compositional gradients in cement pastes. With the goal of preparing homogenous, single-phase C–S–H samples derived from C_3S paste, it was thus important to analyze and minimize the extent of inhomogeneity in the decalcified samples.

Figure 5 shows the variation in solid Ca/Si ratio across the thickness (0.8 mm) of a leached and a recalcified C_3S paste disc. The leached paste had a bulk Ca/Si ratio of 0.83; the recalcified sample was a fragment of the leached specimen equilibrated for three weeks in CH solution (using a solution:solid ratio

of ~ 300), after which time the solid had a bulk Ca/Si ratio of 1.31 and the Ca and Si concentrations in solution equilibrated on solubility curve C of Figure 10 in Ref. [8] at 7.06 mM Ca and 71.3 □M Si.

The leached paste showed a slight gradient in Ca/Si ratio, possessing a value of 0.4 at the surface and ~ 0.8 for a majority of the sample; a few points with Ca/Si ratio of 1.3–1.4 were found near the midline of the sample. Ignoring these high points, the fitted curve for the leached paste suggests that nearly 75% of the volume of the disc possessed compositions within 5% of the measured bulk Ca/Si ratio of 0.83. This level of homogeneity may be adequate in certain studies but not so in cases where precision of the Ca/Si ratio is important.

In contrast to the results of the leached paste, the Ca/Si ratios across the thickness of the recalcified solid were fairly constant, with an average value of 1.22 ± 0.10, close to the measured bulk value of 1.31. Thus, recalcification not only increases the Ca/Si ratio of the solid, but also improves the homogeneity of the sample by removing the compositional gradients induced by leaching. Note that, as illustrated in a previous study [8], the Ca/Si ratio of this recalcified sample could have been lower or higher (within the range of about 0.7–1.8) by adjusting the concentration of the CH solution to which the leached solid was exposed.

As discussed in Section 4, these results demonstrate that homogenous, single-phase specimens with varying Ca/Si ratio can be successfully prepared from C_3S pastes through a combined decalcification and recalcification procedure.

3.6. Changes in porosity and bulk density during decalcification in NH_4NO_3 solution. Figure 6 shows that the porosity (□) and the bulk wet density ($□_{bulk}$) of decalcified C_3S paste increases and decreases, respectively, with decalcification (i.e., with decreasing Ca/Si ratio). The trendlines are valid for C_3S pastes with a water:cement ratio of 0.5.

It is important to note that by the time CH has been fully extracted from the paste at a Ca/Si of 1.4, the porosity is approximately 60%; based on the NIST hydration model [36], this porosity value suggests that the capillary pores of the decalcified paste are completely percolated (or continuous) in 3-dimensions. This percolated pore structure increases the diffusivity of the leached solid by 2 or more orders of magnitude, thus facilitating the exchange of the NH_4NO_3 solution with water and the recalcification of the leached solid in CH solution.

4. Discussion

4.1. Procedure for preparing single-phase C–S–H specimens from C_3S pastes. The results of this study suggest a strategy based on a decalcification/recalcification procedure for preparing homogeneous, single-phase C–S–H specimens from C_3S pastes with varying Ca/Si ratio. This method is outlined here:

1. Prepare thin specimens of a fully-hydrated C_3S paste to reduce leaching times and to minimize compositional gradients during decalcification. A thickness of 0.8 mm produced adequate results in this study. Although decreasing this thickness could possibly produce more homogenous specimens, handling the fragile leached specimens becomes more difficult.
2. Decalcify the paste in concentrated NH_4NO_3 solution at a fairly high solution:solid ratio. A concentration of 6M and a solution:solid ratio of ~ 200 by weight were used here; both of these values, however, can be safely reduced as long as the pH of the leaching solution remains below 9.25, the pH above which decalcification in NH_4NO_3 solution should cease [29].

3. Continue decalcification at least until CH is completely extracted from the C_3S paste; C–S–H will inevitably begin to decalcify before this occurs, and for our sample size, CH was removed at a Ca/Si ratio of approximately 1.4. If preparing specimens at higher Ca/Si ratios, go to step 4; if preparing specimens at lower Ca/Si ratios, continue leaching until the target composition is achieved using as guidelines either the aqueous solution composition or the predetermined relationships between weight loss and Ca/Si ratio such as those shown in Figure 4. The lower limit for the Ca/Si ratio of C–S–H is theoretically 0.67 (when all $Si–O^-$ sites are protonated); below this value, silica gel is present.
4. Remove the NH_4NO_3 solution from the pores of the decalcified sample by immersing the solid in deionized water; due to the percolated pore structure (Section 3.6), only 10–15 minutes were necessary for the sample sizes used here. If small gradients in composition are tolerable, stop here; the bulk Ca/Si ratio of this sample adequately represents the composition of the leached solid. If, however, homogeneity or a higher Ca/Si ratio is desired, proceed with recalcification in step 5.
5. Recalcify the sample through continuous shaking for several weeks in CH solution, the concentration of which depends on the target Ca/Si ratio of the sample. Use as guidelines the relationships shown in Figure 3 of Ref. [8] between the Ca/Si ratio of C–S–H gel derived from C_3S and the Ca concentration in aqueous solution with which the solid is in equilibrium. The final Ca/Si ratio of C–S–H, which can vary between approximately 0.7–1.8, will depend on the initial compositions of the solid and solution as well as the solution:solid ratio (a value of ~ 300 was used here); higher Ca/Si ratio solids could require multiple exposures to saturated or supersaturated solutions of CH. The final composition of the aqueous solution should also be measured for Ca and Si to ensure that the concentrations fall on curve C of Figure 10 in Ref. [8]; this is a good indication that equilibrium has been reached.

4.2. Implications for C–S–H research. The procedure outlined above has important implications for C–S–H research, particularly pertaining to the high Ca/Si ratio C–S–H gel found in cement pastes, whose structure is perhaps the most controversial topic on C–S–H.

The most apparent advantage of the present technique is the ability to produce homogeneous, single-phase C–S–H specimens from C_3S pastes with Ca/Si ratios exceeding 1.5, the apparent limit for most synthetic preparations of C–S–H. Moreover, phase equilibrium results [8] show that the nanostructures of C–S–H derived from C_3S pastes are generally quite different from those of synthetic preparations: at a given Ca/Si ratio above 1.2, for example, C–S–H gel from mature C_3S paste has a higher mean chain lengths and a higher Ca–OH content. Both of these attributes, especially the high Ca–OH content, which was confirmed directly from inelastic neutron scattering (INS) spectroscopy [9], support the conclusion [8, 37] that the nanostructure of mature C–S–H gel in C_3S or cement paste is more closely related to jennite than 1.4-nm tobermorite (i.e., C–S–H(I)). On the other hand, synthetic preparations, especially double decomposition, appear to produce structures more tobermorite-like than jennite-like. Therefore, in order to make progress on understanding the nanostructure of C–S–H gel in cements, it appears that characterization should be performed not on synthetic C–S–H preparations (as the majority of studies have done) but on single-phase samples prepared from C_3S pastes as described here.

Investigations concerned with the interaction of high Ca/Si ratio C–S–H gel in cements with species such as chloride ions, metallic and radioactive waste ions, alkali ions, and polymeric dispersants could also potentially benefit from the preparation technique outlined above. For example, if any of these

species bind to or strongly interact with Ca–OH sites in C–S–H (such as chloride ions [38]), sorption studies on single-phase C–S–H specimens will only accurately reflect the situation in mature cement pastes if the specimen has a correspondingly high content of Ca–OH groups (as is naturally present in the paste). Since synthetic C–S–H preparations generally have low Ca–OH contents [8], it would be more appropriate to conduct sorption studies on high Ca/Si ratio C–S–H preparations derived from C_3S pastes.

Another important aspect of the procedure outlined in Section 4.1 is the ability to prepare homogenous C–S–H specimens with low Ca/Si ratios. This is useful for studying the structure and properties of decalcified C–S–H gel present in water- [26], carbonation- [39], or sulfate-attacked [40, 41] cement pastes. In a recent leaching study [35], for example, it was shown that C_3S and cement pastes shrink due to the in situ silicate polymerization in C–S–H induced by decalcification below Ca/Si ratios of 1.2.

5. Summary

A technique for preparing homogeneous, single-phase C–S–H gel specimens of variable Ca/Si ratio from mature, hardened C_3S pastes is presented (see summary in Section 4.1).

An important advantage of this technique is the ability to prepare single-phase C–S–H specimens with Ca/Si ratios as high as 1.8, thus exceeding the apparent limit of 1.5 for most synthetic preparations of C–S–H and thereby forming specimens whose nanostructures more closely resemble that of C–S–H gel in cement paste. The preparation of these high Ca/Si ratio samples involves two steps: first, thin C_3S specimens are decalcified in concentrated NH_4NO_3 solution to extract CH; second, decalcified (and rinsed) solids are equilibrated in CH solution to increase the Ca/Si ratio of C–S–H and also to remove the compositional gradients induced by leaching. Characterization of these high Ca/Si ratio samples should yield new insight into the nanostructure of C–S–H gel in cement pastes.

Studies on the sorption of species such as chloride ions, waste ions, alkali ions, and polymers onto these high Ca/Si ratio preparations could also yield new insight into the specific interactions between these species and C–S–H gel in cement pastes.

A further advantage of the technique described here is the ability to prepare homogeneous, single-phase C–S–H specimens with low Ca/Si ratios (i.e., below ~ 1.2). This could be useful for durability studies concerned with the structure and properties of C–S–H gel decalcified by water leaching, carbonation, or sulfate-attack.

Acknowledgment. The work was supported by the National Science Foundation under Grant No. CMS-0070922/001.

References

[1] X. Cong, R.J. Kirkpatrick, ^{29}Si MAS NMR study of the structure of calcium silicate hydrate, Advn. Cem. Based. Mat. 3 (1996) 144–156.

[2] X. Cong, R.J. Kirkpatrick, ^{17}O MAS NMR investigation of the structure of calcium silicate hydrate gel, J. Am. Ceram. Soc. 79 (6) (1996) 1585–1592.

[3] I. Klur, B. Pollet, J. Virlet, A. Nonat. C–S–H structure evolution with calcium content by multinuclear NMR, in: Nuclear Magnetic Resonance Spectroscopy of Cement-Based Materials, Springer, Berlin, 1998, pp. 119–141.

[4] P. Yu, R.J. Kirkpatrick, B. Poe, P.F. McMillan, X. Cong, Structure of calcium silicate hydrate (C–S–H): Near-, mid-, and far-infrared spectroscopy, J. Am. Ceram. Soc. 82 (3) (1999) 742–748.

[5] N. Lequex, A. Morau, S. Philippot, P. Boch, Extended X-ray absorption fine structure investigation of calcium silicate hydrates, J. Am. Ceram. Soc. 82 (1999) 1299–1306.

[6] M. Grutzeck, A. Benesi, B. Fanning, Silicon-29 magic angle spinning nuclear magnetic resonance study of calcium silicate hydrates, J. Am. Ceram. Soc. 72 (4) (1989) 665–668.

[7] H. Noma, Y. Adachi, H. Yamada, T. Nishino, Y. Matsuda, T. Yokoyama, ^{29}Si MAS NMR spectroscopy of poorly-crystalline calcium silicate hydrates (C–S–H), in: P. Colombet, A.-R. Grimmer, H. Zanni, P. Sozzani (Eds.), Nuclear magnetic resonance spectroscopy of cement-based materials, Springer, Berlin, 1998, pp. 119–141.

[8] J.J. Chen, J.J. Thomas, H.F.W. Taylor, H.M. Jennings, Solubility and structure of calcium silicate hydrate, Cem. Concr. Res., H.F.W. Taylor Memorial Issue (2004).

[9] J.J. Thomas, J.J. Chen, D.A. Neumann, H.M. Jennings, Ca–OH bonding in the C–S–H gel phase of tricalcium silicate and white portland cement pastes measured by inelastic neutron spectroscopy, Chem. Mater. 15 (3813–3817) (2003).

[10] J.J. Thomas, J.J. Chen, A.J. Allen, H.M. Jennings, Effects of decalcification on the microstructure and surface area of cement and tricalcium silicate pastes, submitted (2003).

[11] E. Bonaccorsi, S. Merlino, H.F.W. Taylor, The crystal structure of jennite, $Ca_9Si_6O_{18}(OH)_6{\cdot}8H_2O$, Cem. Concr. Res., H.F.W. Taylor Memorial Issue (2004).

[12] S. Merlino, E. Bonaccorsi, A.R. Kampf, Tobermorite 14Å: Crystal structure and OD character, in: D. Rammlmair, J. Mederer, T. Oberthür, R.B. Heimann, H. Pentinghaus (Eds.), Applied mineralogy, Balkema, Rotterdam, 2000, pp. 859–861.

[13] I.G. Richardson, G.W. Groves, Microstructure and microanalysis of hardened ordinary portland cement pastes, J. Mater. Sci. 28 (1993) 265–277.

[14] A. Nonat, X. Lecoq., The structure, stoichiometry and properties of C–S–H prepared by C_3S hydration under controlled conditions, in: P. Colombet, A.-R. Grimmer, H. Zanni, P. Sozzani (Eds.), Nuclear magnetic resonance spectroscopy of cement-based materials, Springer, Berlin, 1998, pp. 197–207.

[15] G.W. Groves, S.A. Rodger, The hydration of C_3S and ordinary portland cement with relatively large additions of microsilica, Adv. Cem. Res. 2 (8) (1989) 135–140.

[16] C.M. Dobson, D.G. Goberdhan, J.D. Ramsay, S.A. Rodger, ^{29}Si MAS NMR study of the hydration of tricalcium silicate in the presence of finely divided silica, J. Mater. Sci. 23 (1988) 4108–4114.

[17] A.R. Brough, C.M. Dobson, I.G. Richardson, G.W. Groves, A study of the pozzolanic reaction by solid–state ^{29}Si nuclear magnetic resonance using selective isotopic enrichment, J. Mater. Sci. 30 (1995) 1671–1678.

[18] G. Sun, A.R. Brough, J.F. Young, ^{29}Si NMR study of the hydration of Ca_3SiO_5 and β-Ca_2SiO_4 in the presence of silica fume, J. Am. Ceram. Soc. 82 (1999) 3225–3230.

[19] C. Carde, G. Escadeillas, R. Francois, Use of ammonium nitrate solution to simulate and accelerate the leaching of cement pastes due to deionized water, Mag. Concr. Res. 49 (181) (1997) 295–301.

[20] E.E. Pressler, S. Brunauer, D.L. Kantro, Investigation on the Franke method of determining free calcium hydroxide and free calcium oxide, Anal. Chem. 28 (5) (1956) 896–902.

[21] G.L. Kalousek. Application of differential thermal analysis in a study of the system lime-silica-water, in: Proc. 3rd Int. Symp. Chem. Cem., Cement and Concrete Association, London, 1952, pp. 296–311.
[22] F.W. Locher. Stoichiometry of tricalcium silicate hydration, in: Symposium on Structure of Portland Cement Paste and Concrete, Washington, D.C., 1966, pp. 300–308.
[23] V.S. Ramachandran, Differential thermal method of estimating calcium hydroxide in calcium silicate and cement pastes, Cem. Concr. Res. 9 (1979) 677–684.
[24] H.G. Midgley, The determination of calcium hydroxide in set portland cements, Cem. Concr. Res. 9 (1979) 77–82.
[25] H. Stade, W. Wieker, On the structure of ill-crystallized calcium hydrogen silicates. I. Formation and properties on an ill-crystallized calcium hydrogen disilicate phase (in German), Z. Anorg. Allg. Chem. 466 (1980) 55–70.
[26] P. Faucon, B. Gerard, J.F. Jacquinot, J. Marchand, Water attack of a cement paste: Towards an improved accelerated test?, Adv. Cem. Res. 10 (2) (1998) 67–73.
[27] H. Saito, S. Nakane, Comparison between diffusion test and electrochemical acceleration test for leaching degredation of cement hydration products, ACI Mater. J. 96 (1999) 208–211.
[28] F.M. Lea, The action of ammonium salts on concrete, Mag. Concr. Res. 17 (52) (1965) 115–116.
[29] F.H. Heukamp, F.J. Ulm, J.T. Germaine, Mechanical properties of calcium-leached cement pastes: Triaxial stress states and the influence of the pore pressures, Cem. Concr. Res. 31 (2001) 767–774.
[30] J.J. Chen, The nanostructure of calcium silicate hydrate (Ph.D. thesis), Dept. Materials Science and Engineering, Northwestern University, Evanston, IL, 2003.
[31] J.C. Farinas, P. Ortega, Chemical analysis of portland cement by inductively-coupled plasma atomic emission spectrometry, Analusis 20 (1992) 221–228.
[32] L.E. Copeland, J.C. Hayes, Determination of non-evaporable water in hardened portland-cement paste, ASTM Bull. 194 (1953) 70–74.
[33] R.F. Feldman, V.S. Ramachandran, Differentiation of interlayer and adsorbed water in hydrated portland cement by thermal analysis, Cem. Concr. Res. 1 (1971) 607–620.
[34] R.F. Feldman, Helium flow and density measurement of the hydrated tricalcium silicate-water system, Cem. Concr. Res. 2 (1972) 123–136.
[35] J.J. Chen, J.J. Thomas, H.M. Jennings, Polymerization shrinkage of calcium silicate hydrates during decalcification of cement pastes, in preparation.
[36] D.P. Bentz, E.J. Garboczi, Percolation of phases in a three-dimensional cement paste microstructure model, Cem. Concr. Res. 21 (1991) 325–344.
[37] H.F.W. Taylor, Proposed structure for calcium silicate hydrate gel, J. Am. Ceram. Soc. 69 (1986) 464–467.
[38] A.G. Kalinichev, R.J. Kirkpatrick, Molecular dynamics modeling of chloride binding to the surfaces of calcium hydroxide, hydrated calcium aluminate, and calcium silicate phases, Chem. Mater. 14 (2002) 3539–3549.
[39] G.W. Groves, A.R. Brough, I.G. Richardson, C.M. Dobson, Progressive changes in the structure of hardened C_3S cement pastes due to carbonation, J. Am. Ceram. Soc. 74 (11) (1991) 2891–2896.
[40] A.K. Crumbie, K. Scrivener, P.L. Pratt. The relationship between the porosity and permeability of the surface layer of concrete and the ingress of aggressive ions, in: Proc. Mater. Res. Soc. Symp., Materials Research Society, Pittsburgh, 1989, pp. 279–284.
[41] R.S. Gollop, H.F.W. Taylor, Microstructural and microanalytical studies of sulfate attack. I. Ordinary portland cement paste, Cem. Concr. Res. 22 (1992) 1027–1038.

Figure captions

Figure 1. Leaching kinetics of a C_3S paste decalcified in 6 M NH_4NO_3 solution (_) and of a WPC paste leached in flowing deionized water (_).

Figure 2. Ca (_) and Si (_) concentrations in NH_4NO_3 solutions measured after leaching a series of C_3S pastes. Each pair of points at a given Ca/Si ratio represents concentrations in a different 100-mL solution after the leaching of a single specimen disc. The line represents the theoretical Ca concentration in solution assuming a pure decalcification of the solid (i.e., zero loss of Si).

Figure 3. Removal of CH and the decalcification of C–S–H during the decalcification of a C_3S paste. The bulk Ca/Si ratio of the paste (– –) and the Ca/Si ratio of C–S–H (_, —) are shown. CH, represented by the vertically-hatched area, is removed from the paste at a Ca/Si ratio of approximately 1.4.

Figure 4. Relationship between weight loss, *w*, and Ca/Si ratio for C_3S pastes leached in solutions of 6 M NH_4NO_3. The weight loss is determined from specimens saturated with 6 M NH_4NO_3 solution (solid) or from rinsed specimens saturated with water (dashed).

Figure 5. SEM-EDX results measuring the Ca/Si ratio across the thickness (0.8 mm) of a decalcified (_, _, _) and recalcified (_, _) C_3S paste. The symbols in each series represent different, random traverses.

Figure 6. Changes in (a) porosity and (b) bulk wet density as a function of the Ca/Si ratio of C_3S pastes decalcified in solutions of NH_4NO_3.

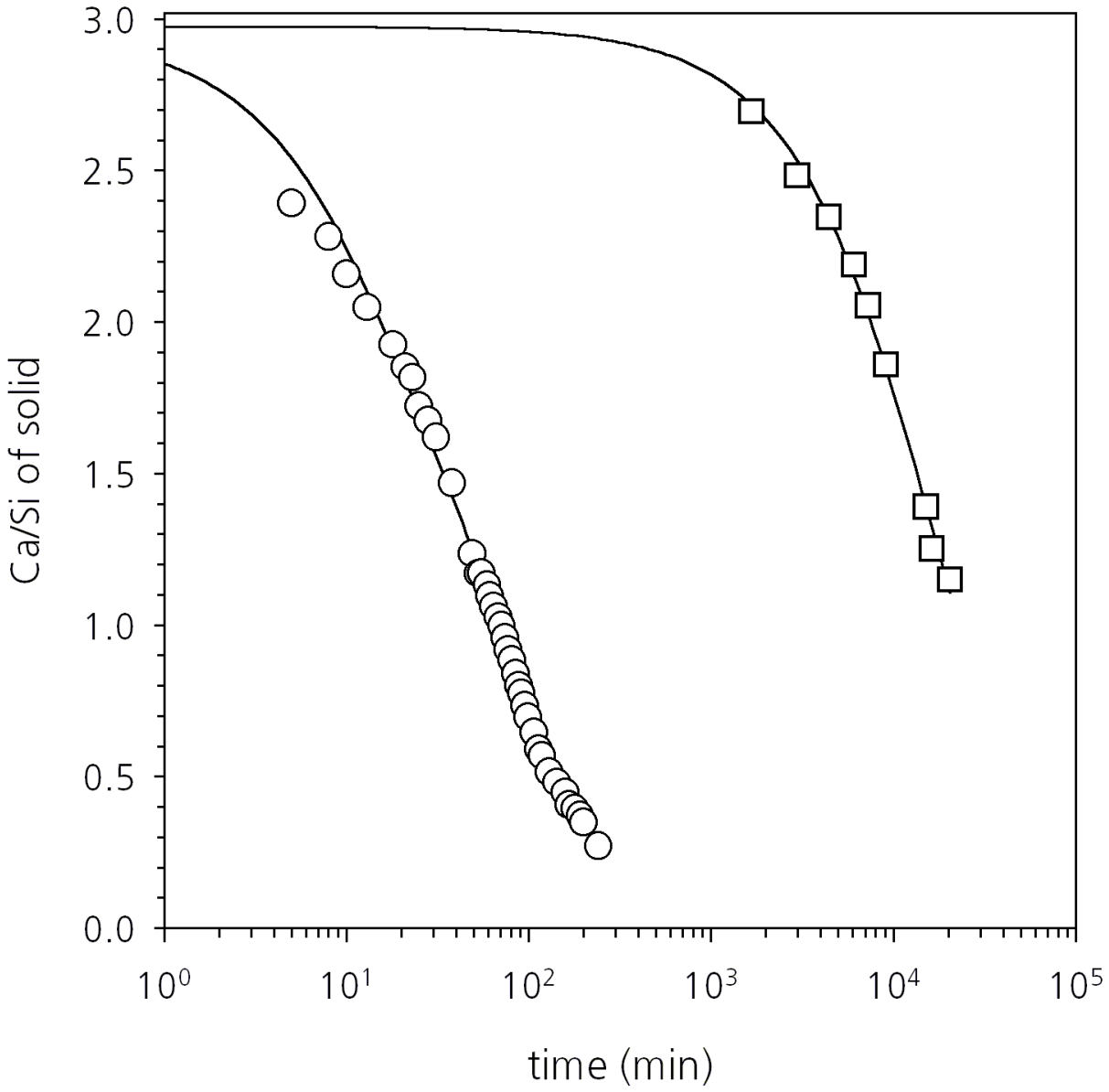
3.0
2.5
2.0
1.5
1.0
0.5
0.0
Ca/Si of solid
10^0
10^1
10^2
10^3
10^4
10^5
time (min)

Figure 1

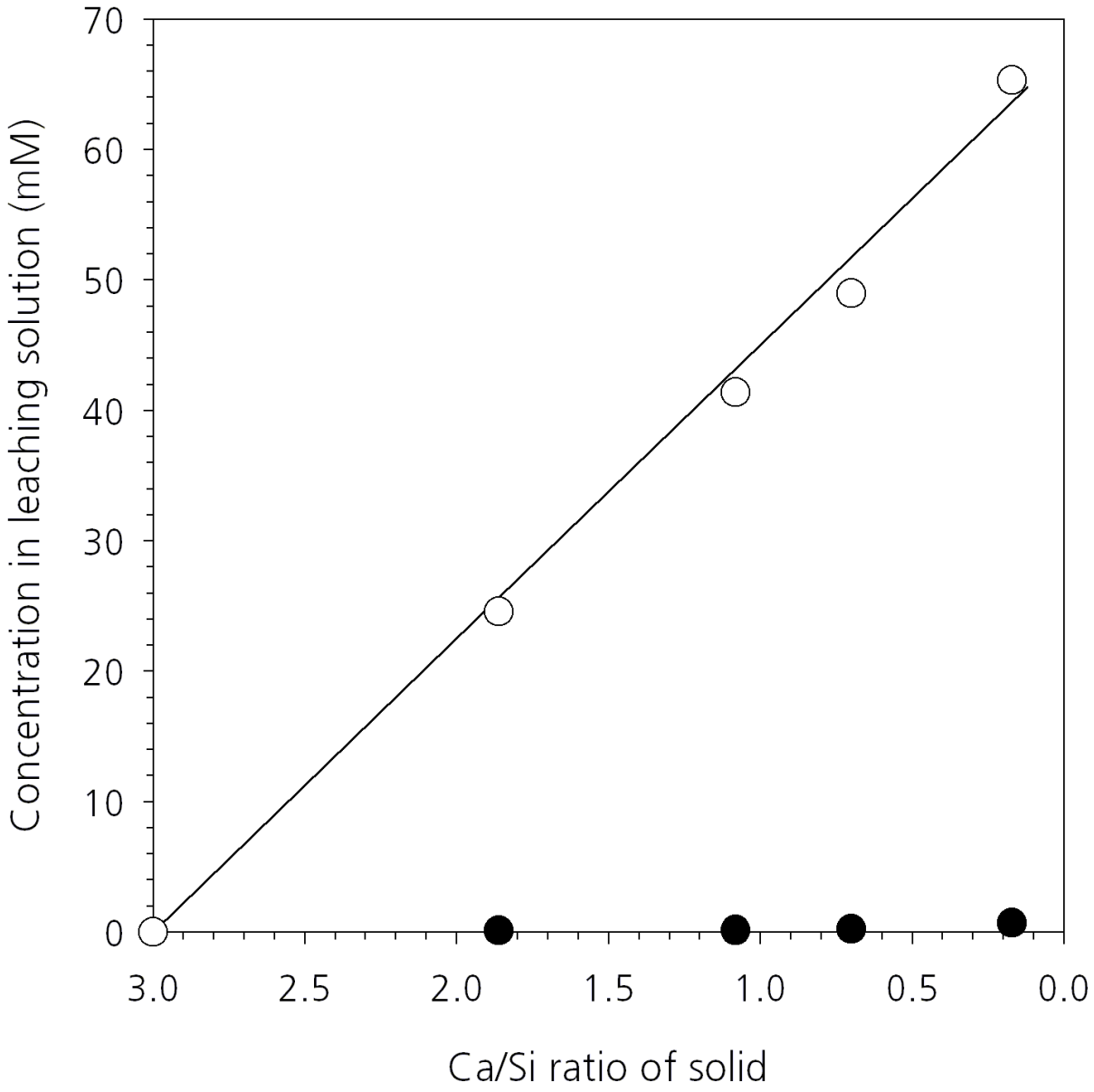
70
60
50
40
30
20
10
0
Concentration in leaching solution (mM)
3.0
2.5
2.0
1.5
1.0
0.5
0.0
Ca/Si ratio of solid

Figure 2

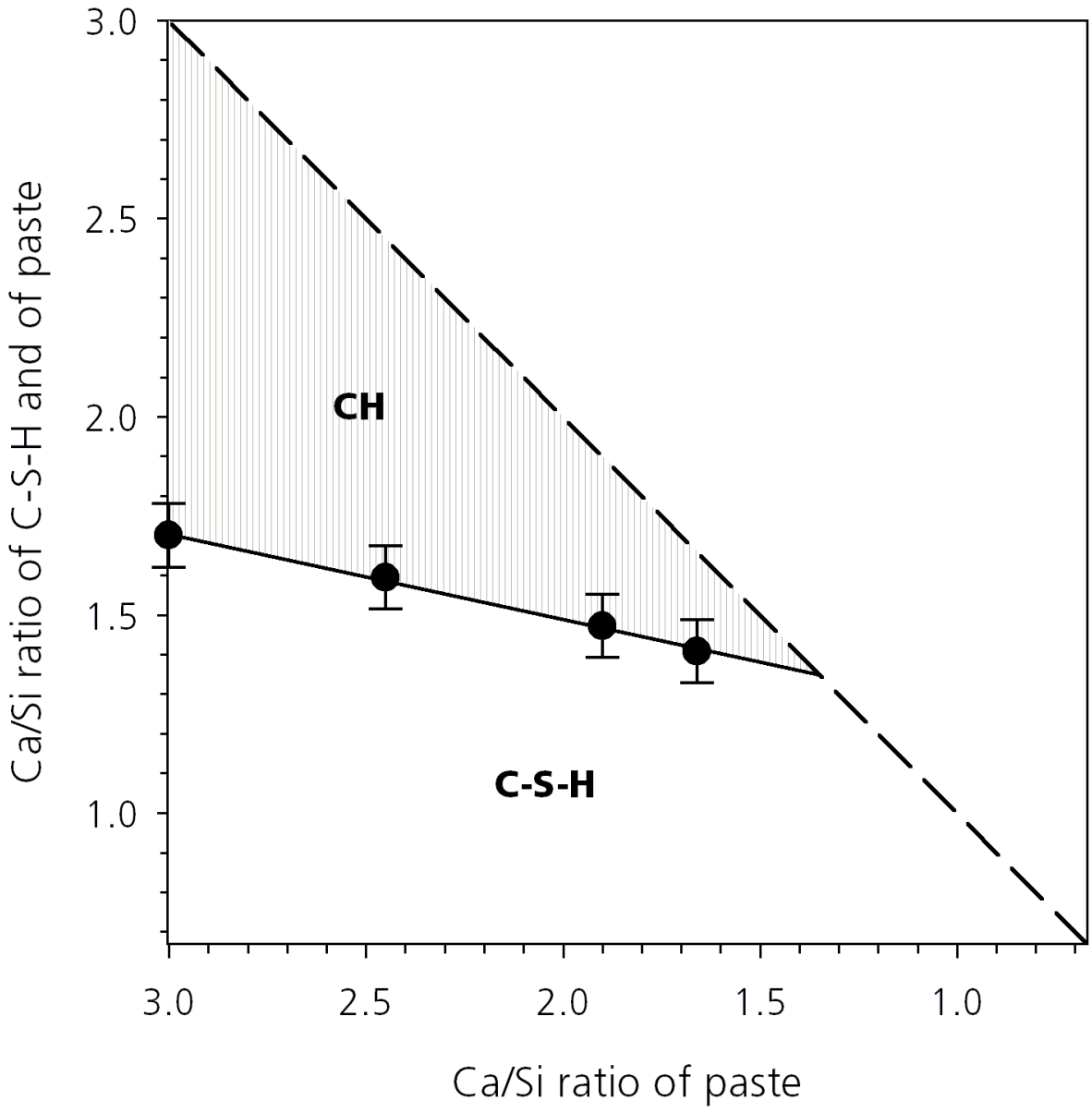
3.0
2.5
2.0
1.5
1.0
Ca/Si ratio of C-S-H and of paste
CH
C-S-H
3.0
2.5
2.0
1.5
1.0
Ca/Si ratio of paste

Figure 3

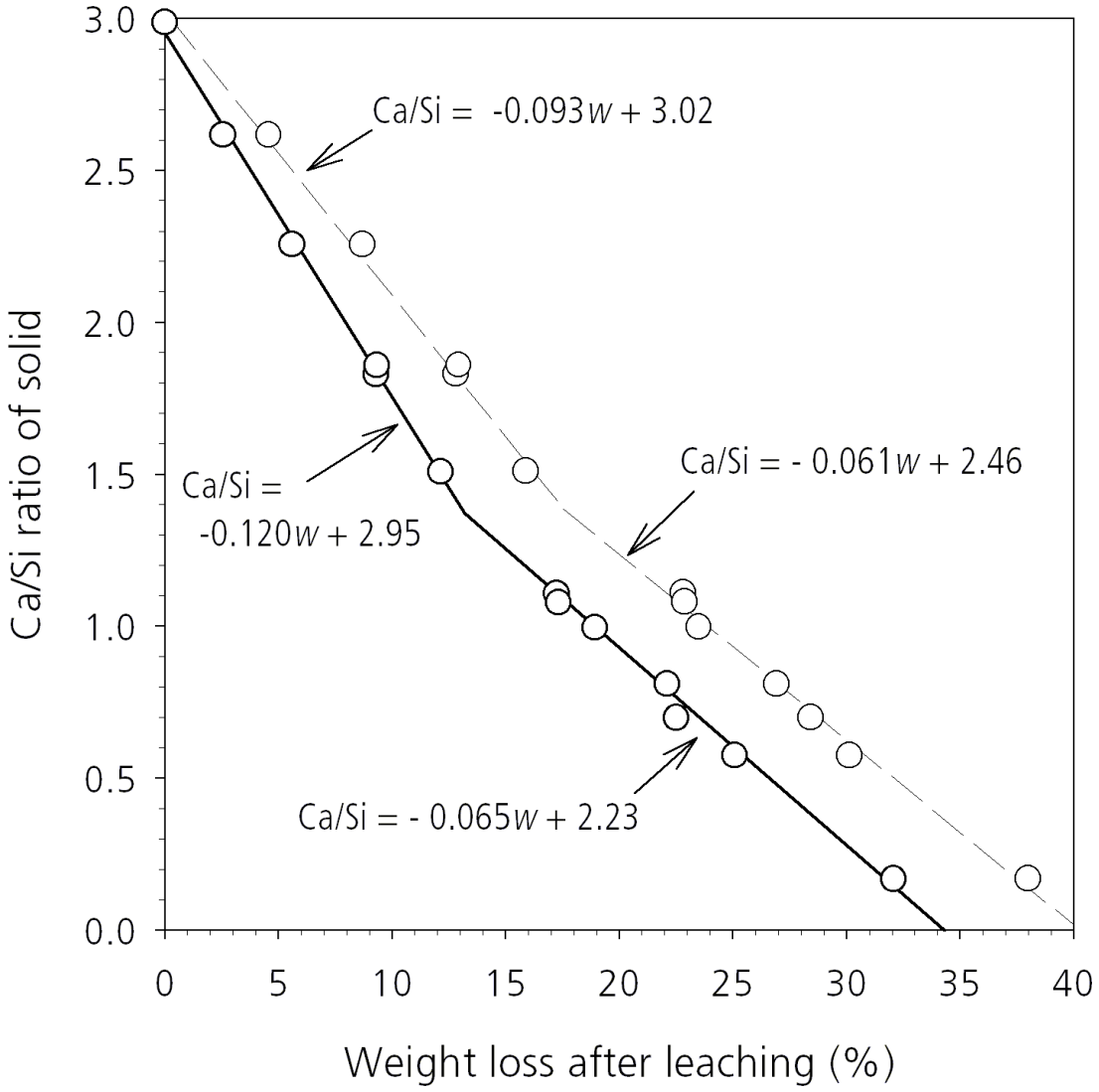
Ca/Si ratio of solid
Weight loss after leaching (%)
Ca/Si = -0.093w + 3.02
Ca/Si = - 0.061w + 2.46
Ca/Si = -0.120w + 2.95
Ca/Si = - 0.065w + 2.23
3.0
2.5
2.0
1.5
1.0
0.5
0.0
0
5
10
15
20
25
30
35
40

Figure 4

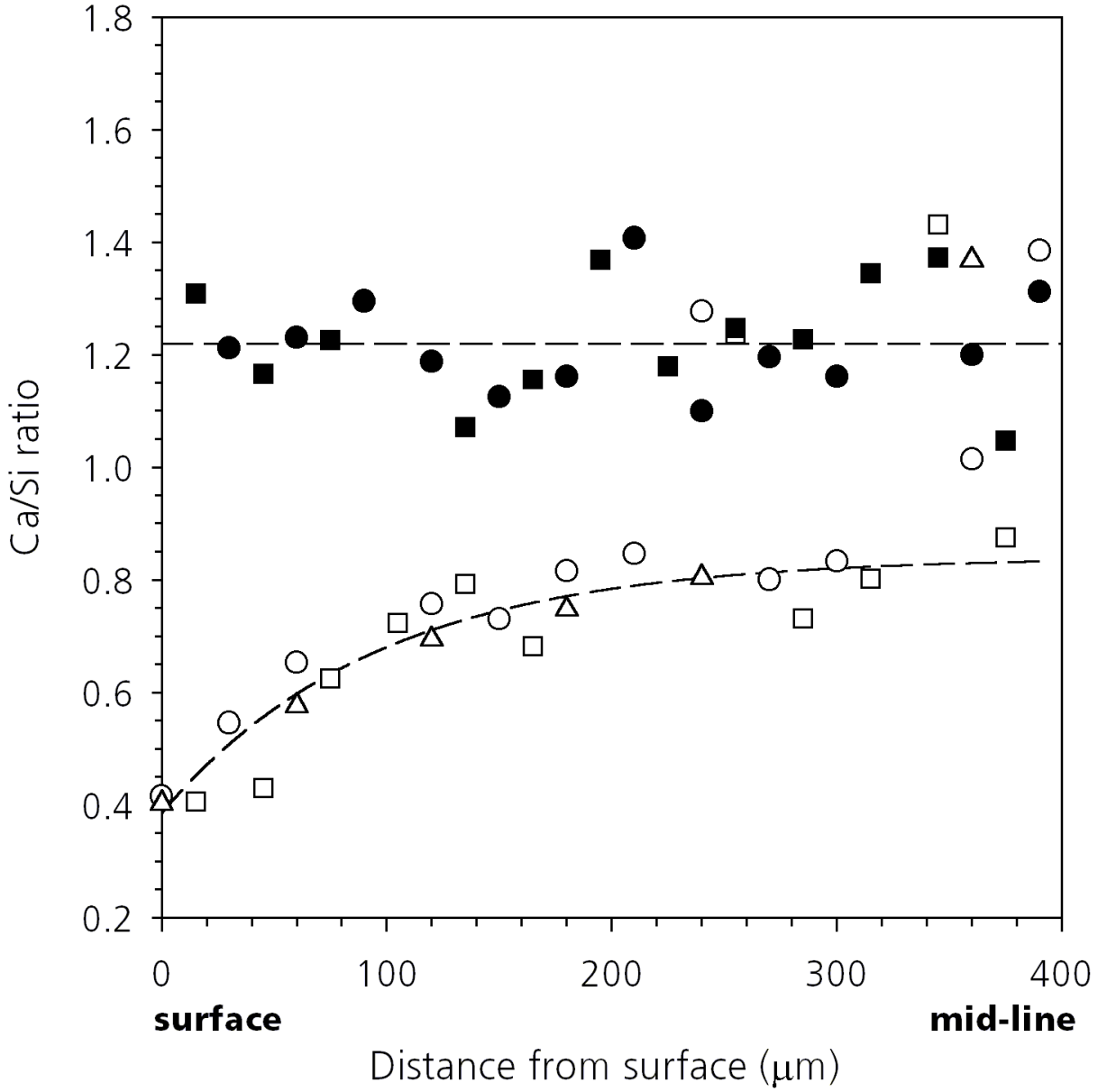
1.8
1.6
1.4
1.2
1.0
0.8
0.6
0.4
0.2
Ca/Si ratio
0
100
200
300
400
surface
mid-line
Distance from surface (μm)

Figure 5

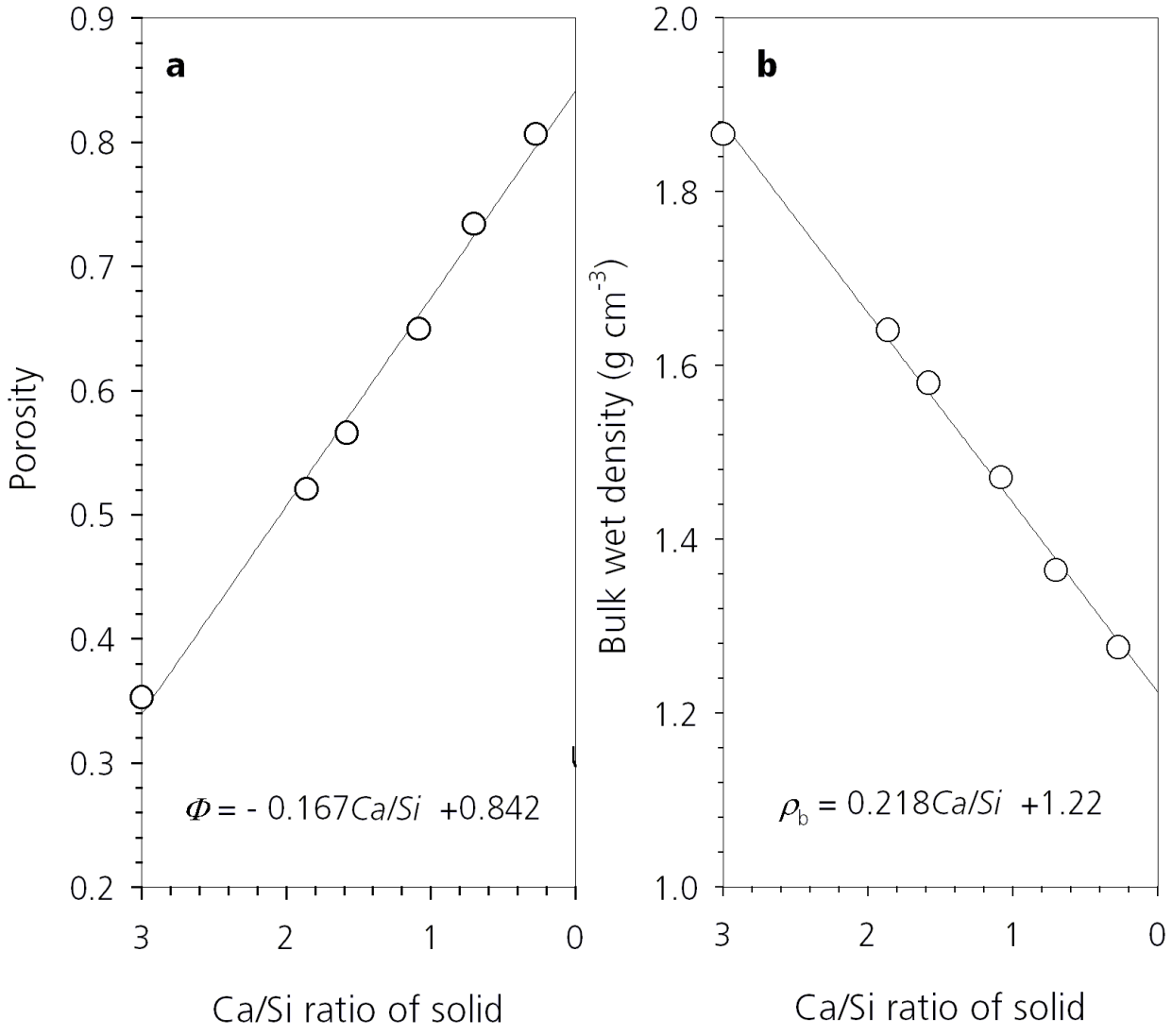
a
Porosity
0.9
0.8
0.7
0.6
0.5
0.4
0.3
0.2
Φ = - 0.167Ca/Si +0.842
3
2
1
0
Ca/Si ratio of solid
b
Bulk wet density (g cm-3)
2.0
1.8
1.6
1.4
1.2
1.0
ρb = 0.218Ca/Si +1.22
3
2
1
0
Ca/Si ratio of solid

Figure 6